

Ozone depletion in Northern Hemisphere winter/spring 1999/2000 as measured by the Global Ozone Monitoring Experiment on ERS-2

K.-U. Eichmann, M. Weber, K. Bramstedt, and J. P. Burrows

Institute of Environmental Physics, University of Bremen, Bremen, Germany

Received 26 July 2001; revised 31 January 2002; accepted 1 March 2002; published 3 October 2002.

[1] During the SOLVE/THESEO 2000 campaign the Global Ozone Monitoring Experiment (GOME) sampled the Arctic region from January to April 2000. Results from the GOME total ozone measurements are presented to highlight the peculiarity of the 1999/2000 Arctic winter/spring season in relation to earlier years. Chemical ozone loss calculations have been derived from daily vortex-averaged ozone profile measurements from GOME. Between 12 February and 13 March 2000, an accumulated chemical ozone loss of 1.3 ± 0.3 ppmv at 475 K isentropic height was derived within the polar vortex. This amounts to a daily chemical depletion rate of 43 ppbv per day (42%). Using 25 January 2000 as a reference date, where six GOME ozone profile measurements were available, an ozone loss of 1.8 ± 0.4 ppmv (49%, 37 ppbv/day) can be derived. The GOME vortex average ozone volume mixing ratios at 475 K agrees well with results from the three-dimensional chemical transport model SLIMCAT and weekly mean values derived from higher-resolution ozone sonde measurements. The low vertical resolution of the GOME measurements leads to an overestimation of ozone after the vortex was split into parts in the middle of March. The accumulated chemical column loss (400–600 K) corrected for diabatic effects is 114 ± 10 DU between 25 January and 13 March. By comparing midlatitude ozone volume mixing ratios from GOME to passive ozone tracer data from SLIMCAT, an ozone loss of about 12% is estimated at 475 K isentropic level within the potential vorticity range between 20 and 30 PVU. This value is statistically insignificant because of uncertainties in model transport. *INDEX TERMS:* 1640 Global Change: Remote sensing; 0340 Atmospheric Composition and Structure: Middle atmosphere—composition and chemistry; 0341 Atmospheric Composition and Structure: Middle atmosphere—constituent transport and chemistry (3334); *KEYWORDS:* GOME, THESEO, lower stratosphere, polar vortex, ozone profile, chemical ozone loss

Citation: Eichmann, K.-U., M. Weber, K. Bramstedt, and J. P. Burrows, Ozone depletion in Northern Hemisphere winter/spring 1999/2000 as measured by the Global Ozone Monitoring Experiment on ERS-2, *J. Geophys. Res.*, 107(D20), 8280, doi:10.1029/2001JD001148, 2002.

1. Introduction

[2] Other methods: Substantial chemical ozone losses, confined to the lower stratosphere, were identified in the Arctic polar vortex from ground based and ozone sonde [see, e.g., Braathen *et al.*, 1994; von der Gathen *et al.*, 1995; Rex *et al.*, 1997; Knudsen *et al.*, 1998a; Sinnhuber *et al.*, 1998], airborne [see, e.g., Proffitt *et al.*, 1993], and satellite measurements [see, e.g., Manney *et al.*, 1996; Müller *et al.*, 1997] during the 1990s. Lower stratospheric winter temperatures are generally higher and more variable in the Arctic than in the Antarctic polar vortex. Thus the formation of polar stratospheric clouds (PSCs) that requires low temperatures, a prerequisite for subsequent chlorine activation and rapid catalytic ozone destruction, becomes

more sporadic. Therefore greater variability in derived Arctic chemical ozone loss rates are observed from year to year. The Arctic winter/spring 1999/2000 falls into the category of cold winter seasons, which were unusually frequent in the middle of the 1990s [Pawson and Naujokat, 1999]. A high number of days where lower stratospheric temperatures were below 195 K, that are required for extensive PSC formation, were observed in 1999/2000 [Manney and Sabutis, 2000]. Difference of the Global Ozone Monitoring Experiment (GOME) total ozone data with modeled passive ozone tracer at the end of March yielded an estimated Arctic vortex chemical ozone loss of about 120 to 140 DU in the total column [Sinnhuber *et al.*, 2000] which was expected as a consequence of observed high chlorine activation [Wagner *et al.*, 2002].

[3] During the SAGE III Ozone Loss and Validation Experiment (SOLVE) and the Third European Stratospheric Experiment on Ozone (THESEO 2000) campaigns between

November 1999 and April 2000, the largest set of satellites, research aircraft, balloons, ozone sondes, and ground-based instruments were combined to study the Arctic stratosphere [Newman *et al.*, 2002]. Different approaches ranging from vortex averaging, tracer methods, and in situ measurements [e.g., Harris *et al.*, 2002; Rex *et al.*, 2002; Hoppel *et al.*, 2002; Bremer *et al.*, 2002; Klein *et al.*, 2002] provides a more coherent picture on the quality of chemical ozone loss estimates. This paper presents chemical ozone loss estimates derived from the height resolved GOME ozone data using a vortex averaging approach. Profile data are retrieved from GOME spectra using a larger wavelength region and a different retrieval scheme as compared to total ozone [Burrows *et al.*, 1999a; Hoogen *et al.*, 1999a]. Chemical ozone loss estimates presented here are based on daily vortex averages centered at the 475 K isentropic level. Diabatic heating rate calculations are included in order to separate dynamical and chemical contribution to the observed ozone change over the course of this winter. The vortex average method is based upon the assumption that dynamical contributions to inner vortex ozone changes are mainly driven by diabatic descent. To show that mixing of extravortex air into the vortex can be neglected, reverse domain filling calculations with an isentropic trajectory model were made. Very little intrusion of midlatitude air into the polar vortex was found. The observed reductions in ozone were thus mainly due to chemistry.

[4] Since GOME is a nadir viewing instrument flying in a near polar sun-synchronous orbit good coverage of the sunlit portion of the polar vortex is achieved. The UV/vis spectrometer GOME measures the backscattered and reflected sun light and therefore polar night observations are not possible. The strength of the GOME observations lies in the late winter and spring period.

[5] Section 2 describes briefly the GOME instrument followed by a summary on ozone retrieval from GOME (section 3). An overview of the total ozone observations in the Arctic between 1995/1996 and 2000/2001 is also presented in this section in order to highlight the THESEO 2000 winter/spring season. Diabatic Ozone change estimates based on radiative transfer calculations are summarized in section 4. The chemical ozone depletion results from GOME in winter/spring 1999/2000 are discussed in section 5. Chemical ozone loss calculations have been carried out using ozone vmr at 475 K isentrope and, alternatively, subcolumns between 400 K and 600 K.

[6] Ozone profile data have been compared with ozone sonde data and results from the SLIMCAT three-dimensional chemical transport model (CTM) showing overall good agreement between the various data sets (section 6) despite the different vertical resolution. Comparisons with results from other SOLVE/THESEO 2000 campaign measurements will also be given. Combining ozone profile data from outside the polar vortex with SLIMCAT passive tracer data an estimate for chemical ozone loss in midlatitudes is

presented (section 7). Concluding remarks are given in section 8.

2. The Gome Instrument

[7] The GOME spectrometer was launched on 21 April 1995 on board the ERS-2 spacecraft. ERS-2 flies in a sun synchronous near polar orbit at a mean altitude of 795 km. The equator crossing time in the descending node is at 10:30am local time. GOME is a nadir viewing UV/visible spectrometer that covers the entire spectrum from 240 nm to 790 nm at a spectral resolution varying between 0.2 and 0.3 nm in four separate spectral channels [Burrows *et al.*, 1999a, and references therein]. The measurement sequence consists of an across-track scan cycle lasting 6 sec, three radiance measurements 1.5 s each in the forward direction covering a maximum surface area of 40 km along track \times 960 km across track and the final back scan. Global coverage is achieved after 42 orbits or approximately three days. At latitudes higher than 65° complete coverage is provided daily except for the polar night region. In the short wave channel of GOME (channel 1a: 240–307 nm before June 1998, currently 240–283 nm) integration time is 12 s leading to a surface area coverage of approximately 100 km \times 960 km for a single radiance measurement. Total ozone derived from channel 2 spectra (1.5 s integration time, surface coverage of 40 \times 320 km²) have therefore higher spatial resolution than ozone profile data which use part of the spectra in channel 1a in their retrieval.

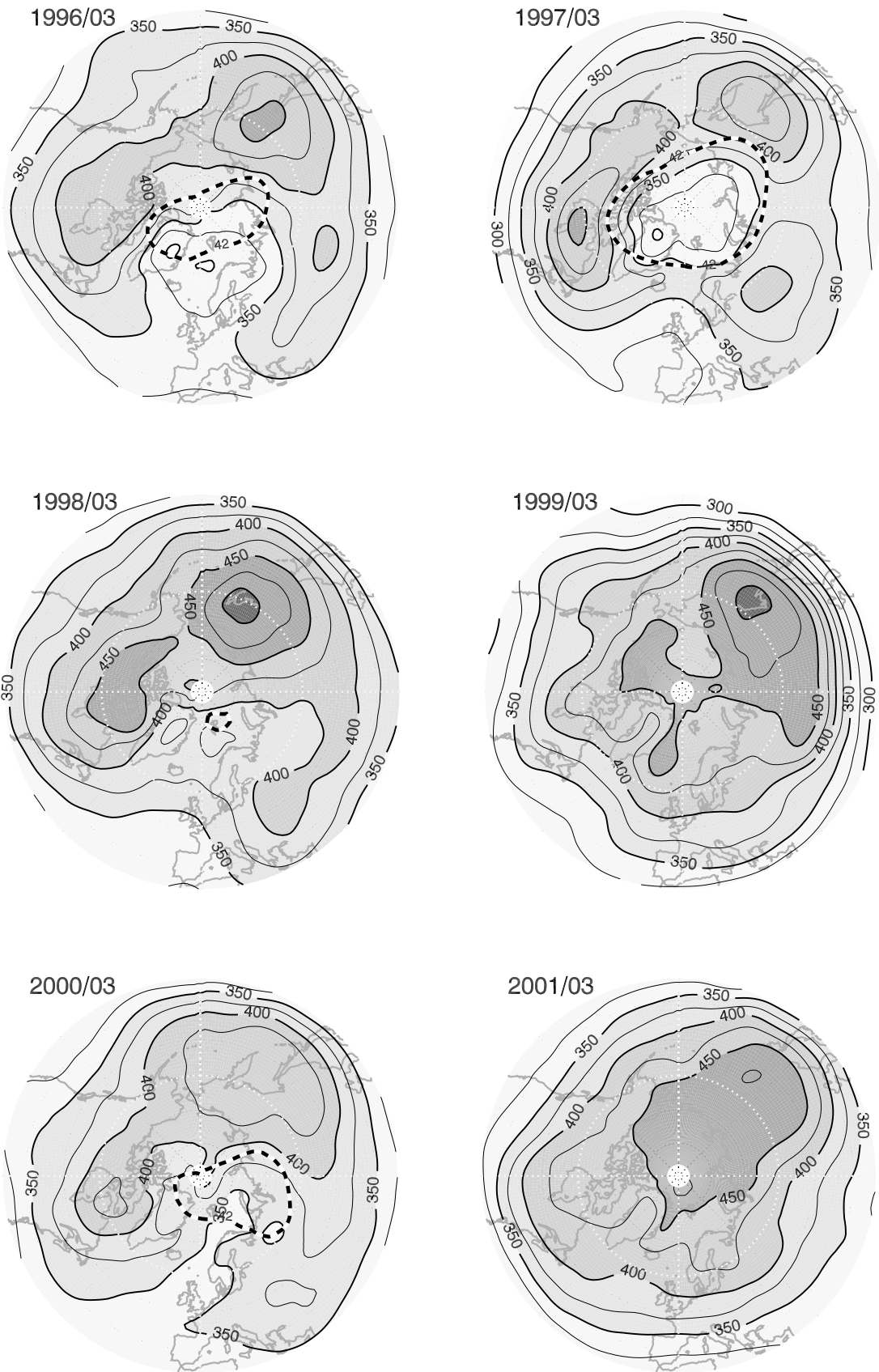
3. Gome Data and Analysis

3.1 Gome Total Ozone 1996–2001

[8] Total columns of trace gases like O₃, NO₂, ClO, BrO, and SO₂ can be retrieved using the differential optical absorption spectroscopy (DOAS) technique [Platt and Perner, 1994; Burrows *et al.*, 1999a; Wagner *et al.*, 2001, 2002]. The total ozone column amount is retrieved in a spectral window between 325 and 335 nm (GOME channel 2) utilizing the measurement of the up-welling radiance and the extraterrestrial irradiance, the latter recorded once a day by directly viewing the sun via a diffuser plate [Weber *et al.*, 1998]. The division of the retrieved slant column by an air mass factor (AMF) determined by radiative transfer calculation yields the total vertical column density [Burrows *et al.*, 1999a]. A correction for the missing column amount below the clouds is applied using the fractional cloud cover information derived from the missing oxygen A band absorption below the cloud top measured at 760 nm [Burrows *et al.*, 1999a].

[9] Total ozone data presented here are from version 2.70 of the GOME Data Processor (GDP). By comparing GDP version 2.00 data with collocated ground based measurements from the Network for the Detection of Stratospheric Change (NDSC) a global agreement to within $\pm 4\%$ was

Figure 1. (opposite) Northern Hemisphere March total column ozone [DU] observed by GOME between 1996 and 2001. The polar stereographic projection extends from 34°N to the pole with 0°E at the bottom. A latitude circle is shown for 60°N. Contour interval is 25 DU. Darker shading indicates larger ozone values. A monthly mean 42 PVU contour line based upon ECMWF potential vorticity (thick dashed line) indicates the average size of the polar vortex at 475 K isentropic level. One potential vorticity unit (PVU) equals 1×10^{-6} K m²/kg · sec.



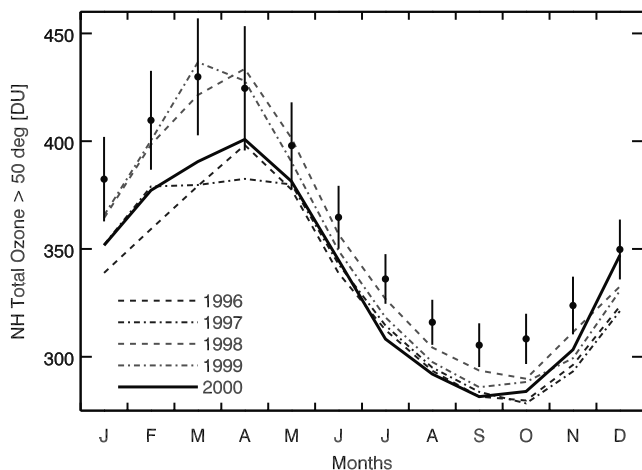


Figure 2. Annual cycle of monthly and zonally averaged column ozone [DU] north of 50°N. The thick black lines mark GOME results for the years 1996–2000. The solid line shows the result for 2000, indicating that 1999/2000 Arctic winter belongs to the series of cold winters (see text). The crosses and error bars mark Nimbus-7 TOMS averages for the pre-Pinatubo period (1979–1991) and the 2σ confidence level, respectively. TOMS data were taken from the TOMS website (<http://jwocky.gsfc.nasa.gov/>).

found [Lambert et al., 1999]. At high solar zenith angles (>75°) larger differences of up to ± 10% have been found. In the polar region GOME overestimates the lowest columns (<260 DU, 1 DU = 2.687 × 10¹⁶ molecules cm⁻²) and underestimates highest columns by an average of 4%. Best agreement is observed around 300 DU [Lambert et al., 1999]. Major changes from GDP version 2.00 and 2.70 were related to the NO₂ total column retrieval with only minor modifications to total ozone data processing.

[10] To give an overview of the total ozone field in winter/spring 1999/2000 with respect to the other winters measured by GOME, Northern Hemispheric maps of March total ozone are plotted in Figure 1 for the years 1996–2001. The mean vortex position at the isentropic surface of 475 K (about 19 km altitude) is indicated by the 42 PVU contour (dashed line) from ECMWF analyses. The March ozone distribution shows strong interannual variability. March 1996, 1997, and 2000 show an extended region with low total ozone in the polar region coinciding with the mean polar vortex position. For these years extended periods of extreme cold stratospheric temperatures were observed in the winter months [Manney and Sabutis, 2000; Pawson and Naujokat, 1999]. In contrast, in 1998, 1999, and 2001 no pronounced local minima in polar total ozone is observed following Arctic winters with considerably warmer temperatures during the preceding winter months. In these winters the polar vortex has weakened considerably by early March as shown by missing or very small vortex areas in Figure 1.

[11] This is further elucidated by looking at the annual cycle of total ozone mean north of 50° shown for all GOME years (1996–2000) in Figure 2. The range of ozone values and its mean derived from Nimbus 7 TOMS version 7 data from the pre-Pinatubo period (1978–1991) are also shown

for comparison. The largest differences to the pre-Pinatubo period are observed between January and April, while during the rest of the year the variability is comparatively small. The Arctic winter 1999/2000 like the other cold Arctic winters 1995/96 and 1996/97 exhibits monthly mean total ozone which are markedly lower than the means in winter and early spring before 1991 (Figure 2) and the GOME data in 1998 and 1999. All summer and early fall GOME monthly means are lower than the pre-Pinatubo data. This can partly be attributed to increased gas phase halogen-catalyzed destruction of ozone throughout the year [Chipperfield and Jones, 1999]. Furthermore midlatitude aerosols as well as changes in dynamics play a substantial role in the midlatitude ozone trends [Hauchecorne and Peter, 2001].

[12] Table 1 summarizes the February and March total ozone north of 50°N, divided up in means calculated inside and outside the polar vortex using 38 PVU at 475 K isentropic level as boundary value. Total ozone is always lower inside the vortex except for the stratospheric warm year of 1999. The chemical ozone depletion can not be discerned from total ozone measurements alone as dynamics plays an important role in the interannual variability of total ozone in the entire Northern Hemisphere as evident in the correlation of the interannual variability of midlatitude and polar vortex total ozone as shown by the data in Table 1.

[13] In March 2000 the total ozone mean of 356 DU inside the polar vortex are close to the March 1996 (335 DU) and 1997 values (351 DU). The particularly low vortex values observed in 1996 (333 DU and 335 DU in February and March, respectively) are associated with quite frequent and extreme ozone mini-hole events at the vortex edge leading to short-term reduction of minimum values below 200 DU in the Arctic [Manney et al., 1996; Weber et al., 2001]. One should note here that March 1997 mean total ozone north of 63° were at a record low in comparison to satellite measurements available since 1979 [Newman et al., 1997]. As in 1995/96 and 1996/97, more than 80 days of minimum lower stratospheric temperatures below 195 K at 50 hPa were observed during the 1999/2000 season [Coy et al., 1997; Pawson and Naujokat, 1999; Weber et al., 2001] (see also Figure 3). In early January polar vortex area reached record levels (circa 23 × 10⁶ km²). A rather fast breakup of the polar vortex was observed after mid to late March.

3.2. Ozone Profile

[14] The short-wave region of the GOME measurements covers the Hartley-Huggins ozone bands and contains

Table 1. GOME Total Ozone Monthly Means [DU] for the Area North of 50°N (All), the Area Between 50°N and the Contour Line of 38 PVU at the Isentropic Height of 475 K (Out), and the Vortex Area Defined by >38 PVU @ 475 K (In)

| Year | February | | | March | | |
|------|----------|-----|-----|-------|-----|----------------|
| | All | Out | In | All | Out | In |
| 1996 | 360 | 369 | 333 | 380 | 391 | 335 |
| 1997 | 379 | 382 | 360 | 380 | 395 | 351 |
| 1998 | 398 | 403 | 363 | 421 | 426 | 394 |
| 1999 | 399 | 396 | 425 | 437 | 436 | 462 |
| 2000 | 376 | 381 | 364 | 391 | 401 | 356 |
| 2001 | 409 | 414 | 383 | 434 | 434 | — ^a |

^a Sample too small or zero.

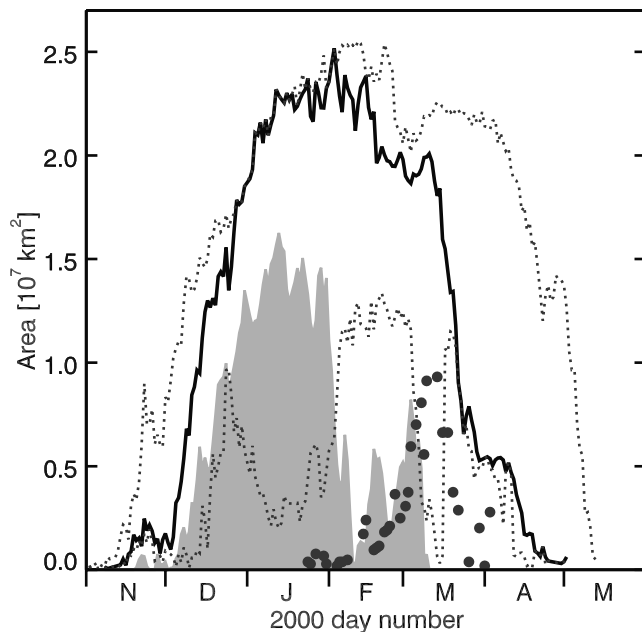


Figure 3. Time series of the vortex area size and the area of potential PSC occurrence as defined by the area of UKMO potential vorticity >38 PVU (thick black line) and temperature <195 K (grey shading) at 475 K, respectively. Also plotted as dotted grey lines are the minimum and maximum vortex area for the GOME years 1996–2000. The daily GOME vortex coverage between February and April 2000 are indicated by black circles.

information about the vertical ozone distribution due to the variation of atmospheric optical depth over several magnitudes of order between 250 nm and 350 nm [Singer and Wentworth, 1957; Chance et al., 1997; de Beek et al., 1997]. The use of an inversion scheme to derive height resolved ozone information from radiances measured by a nadir viewing space instrument has been demonstrated with the SBUV family of sensors [Bhartia et al., 1996]. An advanced technique, here called the Full Retrieval Method (FURM), is applied to GOME.

[15] The retrieval model FURM consists of two parts: (1) the pseudo-spherical, multiple-scattering radiative transfer model GOMETRAN as forward model [Rozanov et al., 1997] and (2) an optimal estimation scheme [Rodgers, 2000] including a priori ozone profiles from a climatological database [Fortuin and Kelder, 1998] and an information matrix approach [Kozlov, 1983; Hoogen et al., 1999a, 1999b] for the iterative inversion scheme.

[16] GOMETRAN is a radiative transfer model optimized for the GOME spectral range. The scalar radiative equation is solved using the finite difference method [Rozanov et al., 1997]. Besides top-of-atmosphere sun-normalized radiances, corresponding weighting functions [Rozanov et al., 1998] are calculated for a given atmospheric state as defined by the vertical number density distribution of trace gases (e.g., ozone, NO_2 , and aerosol) and other geophysical parameters, for instance, surface albedo. Absorption cross-sections of ozone and NO_2 are taken from spectroscopic laboratory measurements with the GOME flight model [Burrows et al., 1998, 1999b]. Aerosol profiles and optical

properties are taken from the LOWTRAN-7 aerosol model [Kneizys et al., 1988]. The earth surface and cloud top are treated as Lambertian equivalent reflecting surfaces. By developing the difference between the iterative solution of the atmospheric state vector (including the ozone profile) to the a priori state vector into an series of eigenvectors with truncation of higher-order terms, the information content contained in the GOME measurements can be reduced to a minimum number of parameters (here the expansion coefficients) to be fitted resulting in a numerically stable retrieval scheme. The latter step is called the information-matrix method. Further details on the FURM retrieval are given in Hoogen et al. [1999a, 1999b].

[17] Extraterrestrial and nadir radiance spectra from GOME (GDP version 2.0) in the wavelength range from 290 to 345 nm are used in the profile retrieval. Strong UV degradation at the shortest wavelengths limits the fit at wavelengths above 290 nm, meaning that the retrieved profile approaches the a priori profile for altitudes above 35 km. This, however, does not affect the lower stratospheric profiles investigated here. Temperature and pressure profiles from the United Kingdom Meteorological Office assimilated data set (UKMO-UARS data set) are part of the retrieval [Swinbank and O'Neill, 1994]. Main fitting parameters are ozone number densities at 71 levels between 0 and 70 km and scaling factors for the surface albedo, the aerosol, and NO_2 number density profile, and the neutral density (here surface pressure), and a constant offset for the temperature profile.

[18] The result from the optimal estimation approach, i.e. the ozone number density vector \mathbf{x} , can be described using the averaging kernel matrix \mathbf{A} :

$$\mathbf{x} = \mathbf{A}\mathbf{x}_t + (1 - \mathbf{A})\mathbf{x}_a \quad (1)$$

where \mathbf{x}_t is the true atmospheric profile and \mathbf{x}_a is the a priori profile needed to stabilize the inversion [Hoogen et al., 1999a]. The full width at half maximum (FWHM) of the averaging kernels (which shows the contribution from other altitudes to a given altitude) can be regarded as a good estimate for the vertical resolution attained. Between 17 and 35 km the FWHM lies between 7 and 9 km. It is higher above and below this altitude range [see Hoogen et al., 1999a, Figure 3].

[19] FURM results have been intercompared with ozone sondes profiles, which were convoluted with the GOME averaging kernels to degrade the sonde vertical resolution to that of GOME [Hoogen et al., 1999b]. For five northern midlatitude to high-latitude sonde stations the GOME ozone number density has a positive bias of about 5% with a root-mean-square (RMS) error of about 10% at 20 km altitude. Dynamical variability in the lower stratosphere over the annual cycle is well reproduced by the GOME measurements as compared with annual sonde measurements [Hoogen et al., 1999a; Eichmann et al., 1999; Hoogen et al., 1999b]. Comparison with global data from HALOE (Halogen Occultation Experiment) aboard UARS show an agreement to within 10% for collocated GOME measurements at 20 km altitude [Bramstedt et al., 2001, 2002].

[20] As already mentioned the GOME measurement technique depends on backscattered solar radiation, and no data are obtained in polar night. The FURM retrieval

is further restricted with regard to the solar zenith angle (SZA). Since June 1998 the upper boundary of the long integration channel has been moved to 283 nm. However, since the signal-to-noise ratio is now rather poor between 283 nm and 300 nm, coadding of subsequent GOME pixels to 12 s is still required for profile retrieval. At SZA larger than 76° the integration time increases to 60 s in GOME channel 1A. Longer integration time at larger solar zenith angle, however, leads to large variation in solar zenith angles across the covered surface area, so that average geometric information for the viewing geometry as used in the current retrieval is not sufficient.

4. Diabatic Descent

[21] Mixing ratios from GOME ozone profiles were calculated prominently on the 475 K isentrope for this paper. The 475 K isentrope lies in the lower stratosphere well below the peak of the ozone mixing ratio. Thus diabatic descent generally tends to dynamically increase the ozone vmr at a constant potential temperature surface. To derive chemical ozone loss rates on isentropes from observed trends, the diabatic descent or ascent of air masses and ozone into the considered isentropic level has therefore to be accounted for. The ozone change on an isentropic surface $\partial O_3^d/\partial t$ due to diabatic ascent or descent is given by

$$\frac{\partial O_3^d}{\partial t} = -Q \left(\frac{p_0}{p} \right)^\kappa \frac{\partial O_3}{\partial \theta}, \quad (2)$$

where Q is the diabatic heating rate, p and p_0 are pressure at the isentropic level and surface pressure, respectively, $\kappa = 2/7$ the ratio of the dry air gas constant to the specific heat at constant pressure, and $\frac{\partial O_3}{\partial \theta}$ is the vertical ozone gradient with respect to potential temperature θ in units of ppmv/K [Braathen et al., 1994; Sinnhuber et al., 1998]. For the diabatic descent correction in the column amount between 400 K and 600 K diabatic ozone change at 600 K minus the corresponding value at 400 K yields the net diabatic change for the column.

[22] For each GOME ground pixel heating rates calculations have been performed using the MIDRAD radiative transfer model [Shine, 1991] with temperature and pressure profiles from the UKMO analyses and stratospheric water vapor profiles from the UARS HALOE climatology [Randel et al., 1998]. Assuming a relative humidity of 60% from the surface up to 400 hPa and a linear decrease to 10% at 200 hPa, tropospheric water vapor profiles are derived from the UKMO temperature data. A constant CO₂ volume mixing ratio of 370 ppmv is assumed throughout the atmosphere and GOME ozone profiles are included in the radiative transfer calculation. The ground albedo is taken to be 0.9, as the Arctic vortex remains mainly over ice, snow

and/or clouds during winter and spring. The influence of clouds is neglected.

[23] After averaging the diabatic ozone change (equation (2)) over the vortex area (>42 PVU at 475 K), the accumulated dynamical contribution to the ozone change can be subtracted from the observed trend to yield the accumulated chemical ozone change with time. The results are presented in section 5. This vortex averaging method has been used in the Antarctic vortex using POAM II satellite data by Bevilacqua et al. [1997] and for ozone sondes by Braathen et al. [1994] and Knudsen et al. [1998a].

[24] Vortex-averaged cooling rates from the microwave radiometer RAM at Ny-Ålesund were compared by Klein et al. [2002] with GOME and SLIMCAT model cooling rates showing good agreement between the three data sets.

5. Chemical Ozone Depletion During Arctic Winter 1999/2000

[25] Northern Hemispheric ($>^\circ\text{N}$) ozone profiles from end of January until middle of April were derived from GOME observations in 2000. Maps of gridded ozone subcolumn amounts in the 15–23 km altitude range are shown in Figure 4 for selected days. Minimum subcolumn amounts of below 100 DU are observed within the vortex region by early March. After middle of March the polar vortex weakened considerably (Figure 3) and became strongly distorted before splitting into three parts (March 19). By early April still low subcolumn amounts of 100 DU are observed within the remnants of the lower stratospheric cyclone. For chemical loss determination ozone volume mixing ratios were interpolated to the 475 K isentropic level. Only GOME ground pixels ($100 \times 960 \text{ km}^2$) lying entirely inside the polar vortex are averaged to form the daily vortex mean. The inner vortex (excluding major part of the vortex edge region) was here defined by the region where potential vorticity was more than 42 PVU at 475 K isentropic level.

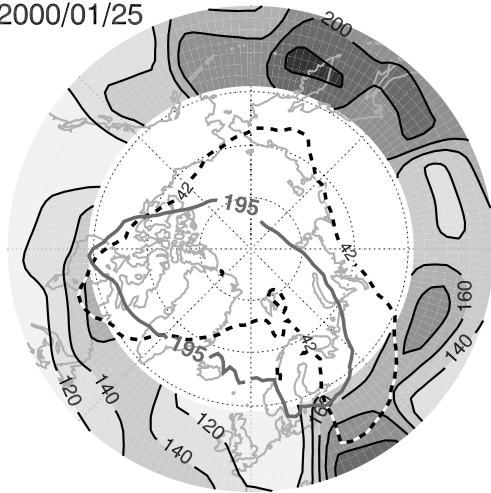
[26] Figure 3 shows the fraction of the vortex area (solid points) for which GOME ozone profiles are available. In general, observation of polar vortex ozone profiles with GOME are possible starting around middle of February. The exact time depends on the actual size of the polar vortex and on how far the vortex is shifted southwards. Because of cyclonic flow of polar air masses a larger part of the polar vortex is, however, actually probed by GOME as indicated in the figure. As the sun returns to the Arctic region in spring, polar coverage steadily improves.

5.1. Ozone Loss at 475 K

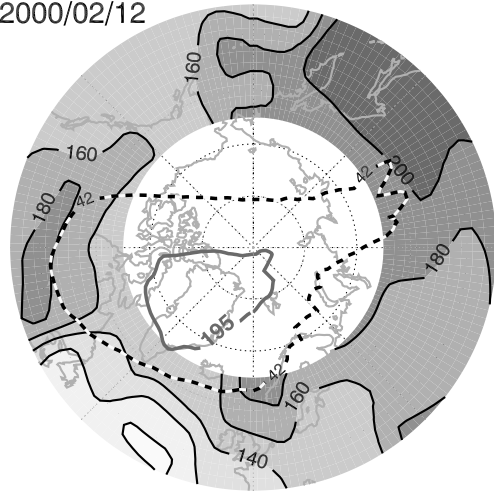
[27] In Figure 5 mean vortex ozone mixing ratios at 475 K inside the polar vortex (>42 PVU) are shown as a time series. Error bars indicate the 1σ standard deviation from taking the mean. The isentropic exchange of air from and

Figure 4. (opposite) GOME subcolumn ozone amounts [DU] for the 15–23 km altitude range for selected days during the period January to April 2000. The stereographic projections start at 45°N with 0°E at the bottom. Contour interval is 20 DU. Darker shading indicates larger ozone values. The dashed line is the 42 PVU contour of ECMWF PV defining the extent of the polar vortex interior region. The thick grey line is the 195 K ECMWF temperature contour (approximate PSC type 1 existence threshold). From top left to bottom right following dates are shown: 25 January, 12 February, 1 March, 13 March, 19 March, and 1 April 2000.

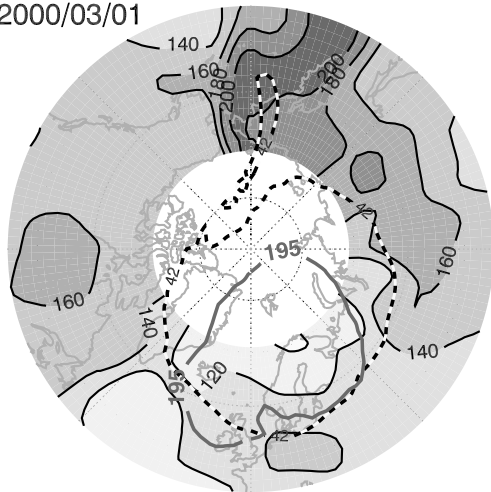
2000/01/25



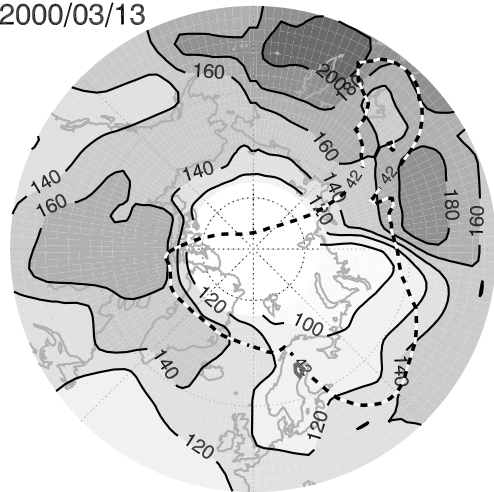
2000/02/12



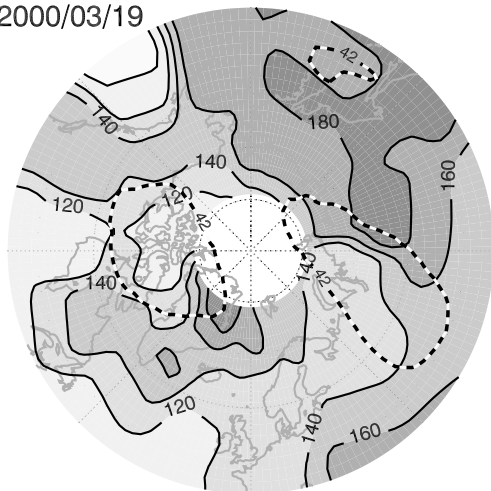
2000/03/01



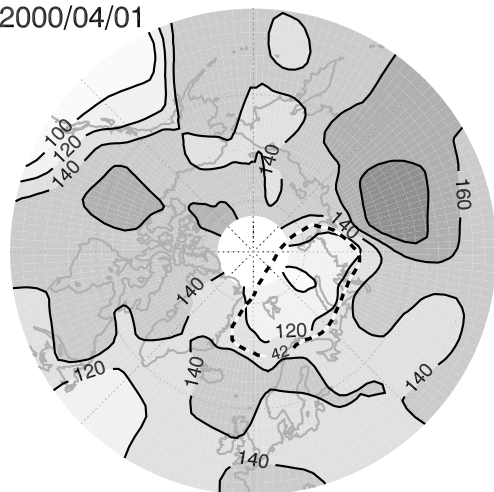
2000/03/13



2000/03/19



2000/04/01



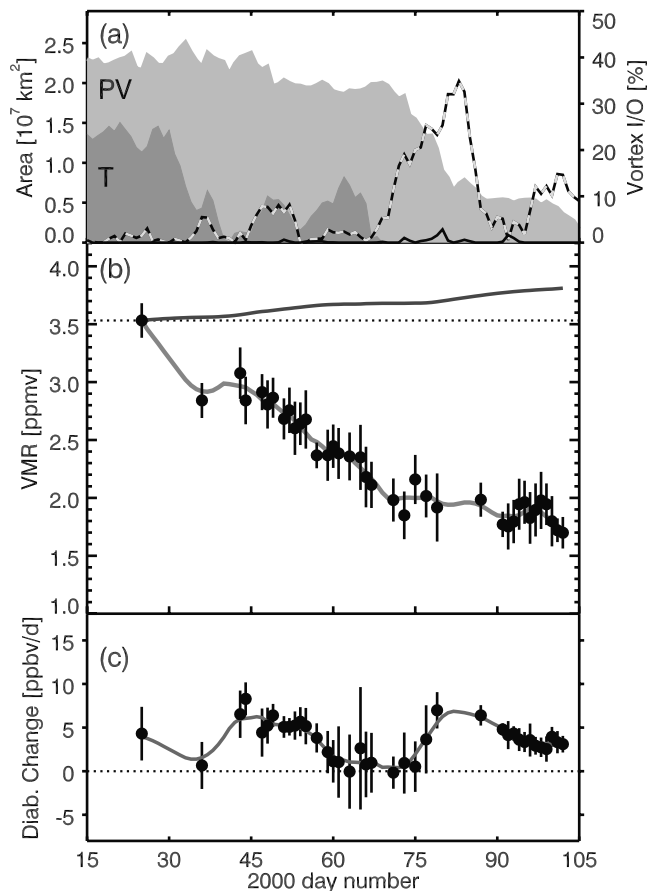


Figure 5. (a) Vortex area [10^7 km^2] (light grey shaded area) and area of possible PSCs ($T < 195 \text{ K}$, dark shaded area) at 475 K. The cross-isentropic exchange of vortex air across the vortex edge using reverse domain filling trajectory calculations with UKMO wind and potential vorticity fields at 475K is shown by the two lines. The percentage of vortex air that is eroded off the vortex as defined by a change from values higher than 42 PVU to less than 30 PVU over the course of 10 days (black/white line). The amount of air entering the polar vortex (change from values below 30 PVU to values larger than 42 PVU) expressed as percentage of the total polar vortex area is shown by the black line. The backward trajectories for the calculations started on a $1^\circ \times 1^\circ$ grid from 35°N to 89°N . (b) Time series of FURM vortex ozone averages [ppmv] (solid circles) and standard deviations at 475 K isentropic height for the winter/spring period 1999/2000. The light grey solid line is a cubic spline interpolation through the five-point running mean. The inner vortex is defined to be inside of the potential vorticity contour line of 42 PVU. Accumulated ozone from diabatic descent is shown by the dark grey solid line starting on 25 January and increasing to the right. (c) Daily ozone increase [ppbv/d] due to diabatic descent averaged over all GOME pixels inside the vortex are displayed. A cubic spline interpolation through the five-point running mean yields the solid and dashed line.

into the vortex at the 475 K isentropic level is shown in the top part of Figure 5. Reverse domain filling (RDF) isentropic trajectory calculations using UKMO data were performed to determine the amount of air leaving the vortex as defined by the 42 PVU contour into middle- to high-latitudes defined by less than 30 PVU and vice versa. Air masses have been exchanged if the actual PV value located at the end of the trajectory differs from its initial PV value [Sobel *et al.*, 1997]. The percentage of vortex area accumulated over 10 days of trajectory lifetime is shown as a time series.

[28] Generally very little amounts of air enters the vortex after the build-up in November/December (not shown here). During dynamically active periods like after the break up of the vortex into three parts as observed in the second half of March small amounts of midlatitude air masses can be injected into the polar vortex. Extrusion of chemically activated vortex air into midlatitudes becomes, however, stronger towards the end of the winter. The relative isolation of the vortex air was also shown by Rex *et al.* [2002] by comparing accumulated ozone loss from Match analysis and from a vortex-averaged approach.

[29] Between 12 February (day 43) and 13 March (day 73) ozone vmr decreased from 3.08 ppmv to 1.85 ppmv. Adding the accumulated diabatic ozone change of about 0.1 ppmv to these results, a polar vortex ozone loss of 1.3 ± 0.3 ppmv (42%) can be derived. This corresponds to an overall loss rate of about 43 ppbv per day. Highest loss rates of more than 45 ppbv/d were reached at the end of February and beginning of March.

[30] Over 1100 ozone profiles were measured inside the vortex for 45 days in the winter/spring period 1999/2000. Before 12 February GOME ozone profile data within the confines of the polar vortex are rather sparse. Two additional days were found with at least six ozone profile measurements fulfilling the criteria of being entirely inside the polar vortex (>42 PVU). These were the days 25 January (see Figure 4), and February, 5, that are also shown in Figure 5.

[31] Selecting 25 January (day 25) as a starting point (mean ozone vmr of 3.530.3 ppmv) a net change of 1.68 ppmv until 13 March is derived. Adding the accumulated diabatic ozone change (0.15 ppmv) a total chemical ozone loss of about 1.8 ± 0.4 ppmv at the 475 K isentropic level can be found from GOME for this period. Because this calculation relies on only six measurement points for one GOME orbit over Russia (Figure 4), larger uncertainties have to be assigned to this value. Inhomogeneities in the ozone amount inside the vortex can cause this high value [Harris *et al.*, 2002]. As shown in section 6, the 3.53 ppmv ozone vmr observed by GOME on 25 January is, however, at the upper limit of individual sonde observations and other measurements from that period.

[32] Between 25 January and 13 March an average depletion rate of 37 ppbv/d is derived from GOME observations. In the second half of March, no O_3 profile data with the above criteria were available. During this period the polar vortex started to erode quickly and lost size as shown in Figures 3 and 4. After early April the polar vortex ozone vmr shows a small increase which is larger than expected from diabatic descent.

[33] Although agreement between GOME and sonde vortex average vmr at 475 K is good, one has to be reminded

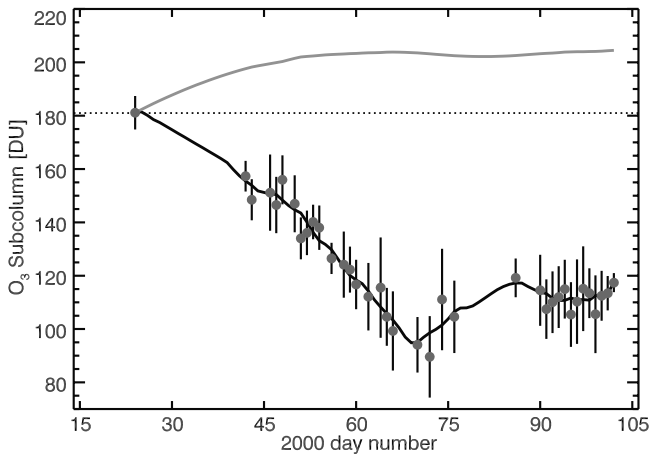


Figure 6. Time series of the 400–600 K GOME subcolumn ozone amounts [DU] inside the polar vortex (>42 PVU @ 475 K) for the period January to April. The grey solid line marks the increase of ozone in the subcolumn due to diabatic descent.

that the vertical resolution is only about 7–9 km for GOME. The vertical resolution at 475 K is about 8 km corresponding to a layer of ± 100 K potential temperature around the 475 K level [Hoogen *et al.*, 1999a]. For this reason, loss estimates for subcolumn amounts between 400 K and 600 K will be presented and discussed in the next section.

5.2. Column Ozone Loss at 400–600 K

[34] A different approach to estimate the overall ozone loss is to calculate the subcolumn ozone [DU] within a certain range of isentropes. Here we have chosen the range from 400 to 600 K, as this is the layer where nearly all ozone loss occurred during the Arctic winter 1999/2000 [Rex *et al.*, 2002; Harris *et al.*, 2002]. The results are shown in Figure 6. A strong decrease in column ozone was found for February and the first half of March down to 90 DU on 13 March. After the vortex split up in three parts in the middle of March, the column amount increases to values around 115 DU in the first half of April. Corrected for the diabatic vertical movement of air into and out of the column and the resulting change of ozone vmr, an accumulated maximum chemical loss of ozone of 114 ± 10 DU for the period from 25 January to 13 March 2000 was found. Compared with GOME total ozone (see Table 1), this is about one third of the total column for March. Again, it should be noted, that the value of 181 DU on 25 January might be over estimated due to a sampling bias in the vortex edge region. The accumulated chemical column loss (400–600 K) corrected for diabatic effects is 73 ± 11 DU between 12 February and 13 March.

[35] Initial comparisons with Match analyses from ozone sonde data show general agreement within the error ranges. Rex *et al.* [2002] found a chemical column ozone loss between the limits of 14 and 24 km of 117 ± 14 DU between early January and late March. SAOZ/REPROBUS measurements show a loss of 105 DU for the whole column between 2 January and 25 March 2000 and POAM profile data with REPROBUS passive ozone show a loss of 80 DU for the partial column 380–700 K [Harris *et al.*, 2002].

These latter value is somewhat lower than the subcolumn ozone observed by GOME.

6. Comparison With Ozone Sondes and the SLIMCAT CTM

[36] A comparison of the GOME results with 7-day running mean of 475 K ozone sonde vmr is shown in Figure 7. The 2σ standard deviations of the GOME measurements are also shown as error bars. The scatter of the individual sonde measurements are of the same order as the standard deviation observed with GOME, so that we can conclude that expect for the second half of March, the agreement between sonde and GOME averages is very good. After day 75, during the second half of March 2000 the vmr of the sonde measurements are systematically lower than GOME. During hisperiod the polar vortex started to erode and split into three parts. A possible explanation for the higher GOME values is the lower vertical resolution of about 8 km of the GOME profiles, meaning that contribution of higher or lower altitude levels not necessary belonging to the polar vortex because of horizontal shearing in the vertical vortex structure may lead to higher observed GOME vmr. Furthermore, the vertical extent of the ozone loss was limited to a small region in the lower stratosphere around 450 K [Rex *et al.*, 2002] and can thus not fully be resolved by GOME.

[37] The vortex ozone measurement result from 25 January is again plotted in Figure 7. GOME tends to over-

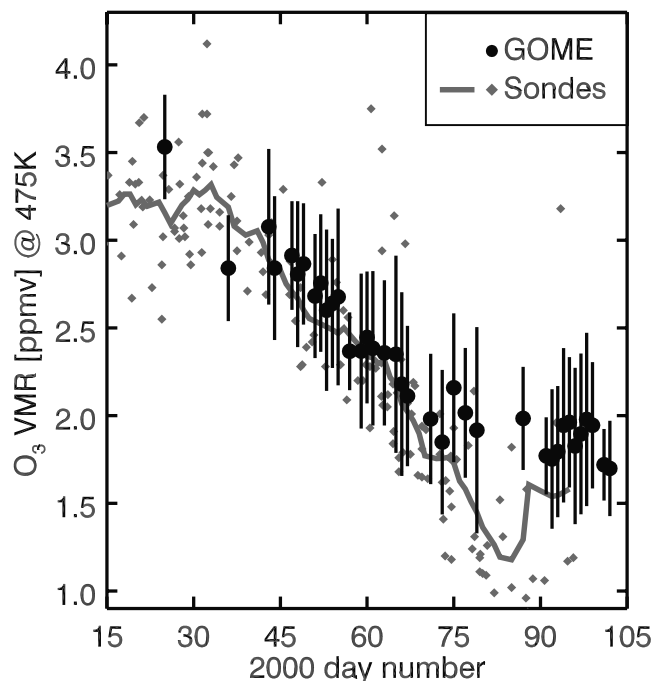


Figure 7. Comparison of the 475 K ozone vmr with ozone sondes measurements inside the polar vortex as defined by 42 PVU at the 475 K isentropic level. The solid black dots mark the daily GOME means and the error bars the 2σ standard deviation. The diamonds mark individual ozone sonde measurements, while the solid grey line gives the 7-day running mean of ozone sonde results.

estimate the 7-day running mean of the sondes by about 0.3 ppmv. Other measurements also show slightly lower vmr of about 3.2 ppmv (RAM, 475 K) [Klein *et al.*, 2002], 3.3 ppmv (AROTEL/DIAL, 450 K) [Lait *et al.*, 2002], and 3.4 ppmv (POAM III, 500 K) [Hoppel *et al.*, 2002]. The overestimation of the vortex average by GOME is due to the fact, that only the outer parts of the inner vortex are probed at the beginning of the measurements. Using the sonde running mean as a starting point for the observed GOME ozone loss calculation, the accumulated chemical ozone loss at 475 K isentropic level would be reduced by 0.3 ppmv to 1.5 ppmv for the period 25 January to 13 March. On the other hand, by mid-March sonde values were also lower than GOME so that accumulated chemical ozone loss with sonde and GOME measurements should be comparable. Because there were only six GOME measurements on one orbit available in late January an uncertainty in the accumulated chemical ozone loss for the January–March period should be conservatively estimated to be 0.4 ppmv, which includes uncertainties from diabatic change calculations.

[38] Comparisons with other measurements from the SOLVE/THESEO 2000 campaign show good agreement as well in total ozone loss as in ozone loss rates. Most loss estimates are in general agreement with losses of about 1.5 to 2.0 ppmv at 475 K by the middle of March [Newman *et al.*, 2002]. A strong decrease in ozone vmr at the beginning of February was also found by POAM III [Hoppel *et al.*, 2002], as the rather sparse GOME data at this time indicates. Klein *et al.*, [2002] have calculated vortex averaged ozone loss rates using RAM measurements from Ny-Alesund. This analysis leads to a maximum ozone loss rate for February and March of 35 ppbv/d, which is also found from GOME measurements. An average ozone loss rate from mid-January to mid-March of 30 ppbv/day was found by Lait *et al.*, [2002] from ozone observation of the AROTEL and DIAL lidars and ozone sondes near 450 K, which was also found by GOME at this height.

[39] The SLIMCAT chemical transport model [Guirlet *et al.*, 2000; Sinnhuber *et al.*, 2000] has a resolution of 2.5° latitude \times 3.75° longitude (approximately 275 km \times 170 km). It is run on 24 isentropic levels from 330 K to 3000 K (approximately 10 to 55 km) with a resulting vertical spacing of one km in the lower stratosphere. The seasonal run used here has been initialized on 1 November using the output of the low-resolution multi-annual integration of the same model, which has been started in October 1991 [Chipperfield, 1999]. Horizontal winds and temperatures are specified from UKMO analyses. The vertical (diabatic) motion is calculated using the same radiation scheme MIDRAD [Shine, 1991] as described earlier. SLIMCAT includes a heterogeneous chemical reaction scheme simulating chemistry on the surface of PSC particles and a simple parameterization to account for sedimentation of PSC particles, which are responsible for strong denitrification processes [Chipperfield and Pyle, 1998; Waibel *et al.*, 1999]. Passive ozone, which is ozone without chemical change advected with the model is initialized on 1 December. Differences between the passive ozone tracer and the CTM ozone provides an estimate of the modeled chemical ozone loss [Sinnhuber *et al.*, 2000].

[40] In Figure 8 the evolution of daily mean ozone vmr inside the Arctic vortex as observed by GOME and by the

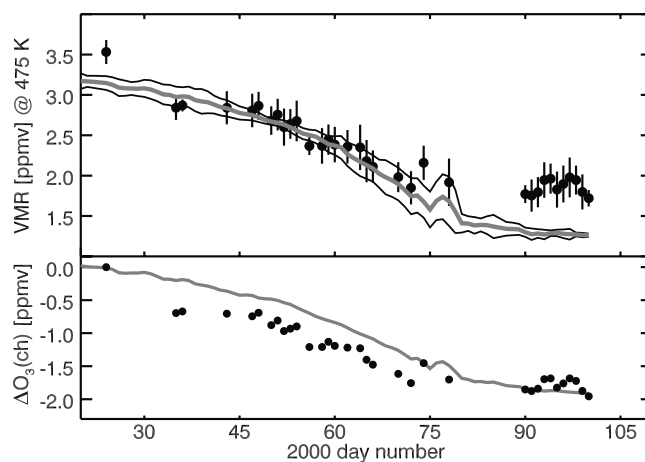


Figure 8. (top) Comparison of GOME vortex average ozone [ppmv] with SLIMCAT model data at 475 K in late winter/spring 2000. GOME observations are the solid points with 1σ error bars, while SLIMCAT ozone averages and the 1σ scatter are shown by thick and thin solid lines, respectively. (bottom) Accumulated chemical ozone loss at 475 K isentropic height from GOME (solid circles) and SLIMCAT (solid line). The GOME chemical ozone change was derived by subtracting diabatic increases from the ozone vmr means shown in top. Reference date for both GOME and SLIMCAT data is January, 25. SLIMCAT results have been obtained by subtracting averaged passive tracer ozone changes from the vortex averages.

SLIMCAT model is shown. In general excellent agreement between the model and GOME observations is found, except for the 25 January GOME ozone mean that is about 0.3 ppmv larger than the SLIMCAT value and the early April period, where GOME is about 0.5 ppmv higher than SLIMCAT. The evolution of accumulated chemical ozone loss is shown in the bottom of Figure 8, showing that up to mid-March just before the splitting of the polar vortex into several parts both modeled and observed chemical ozone losses are in good agreement. An accumulated chemical loss of 1.7 ppmv is estimated from model calculation during the period from 1 December to 19 March. This compares well to the 1.8 ppmv chemical ozone loss observed by GOME, that was, however, derived from the shorter period starting 25 January. Setting the accumulated chemical ozone loss from SLIMCAT to zero on 25 January leads to a 1.4 ppmv modeled accumulated loss until mid-March. While the January value is too high, the vmr on 5 February was too low. This leads to an unrealistically high ozone loss in January/February. Another effect could be the sampling bias due to solar illumination changes in the vortex edge region. This was observed by Schoeberl *et al.* [2002] by comparing POAM and ozone sonde data. Instruments that require sunlight like GOME and POAM do not measure the polar night region of the vortex and thus tend to overestimate the ozone loss early in the year, where a large part of the vortex can not be seen.

[41] Similar to the comparison with ozone sondes, deviations between GOME and SLIMCAT in vmr and accumulated ozone loss are observed after middle of March. This is again most likely due to the vertical resolution in the GOME

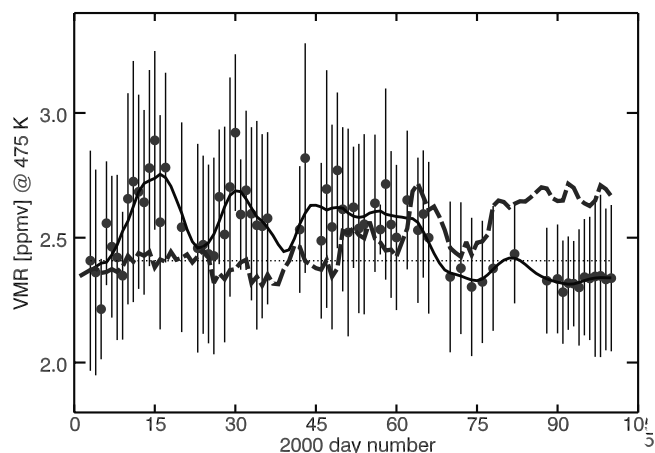


Figure 9. Time series of FURM ozone means and standard deviation for the potential vorticity range from 20 to 30 PVU. The solid line is the cubic spline interpolated five-point running mean. The SLIMCAT passive ozone for the same PV range is shown by the dashed line. The time series covers the period 4 January (day 4) to 10 April (day 100). On 10 April 2000 the difference between GOME and SLIMCAT (0.3 ppmv) can be interpreted as chemical ozone loss in the 20–30 PVU range.

measurements being lower than that of the model, while the ozone loss is restricted to a small vertical region. One should note here that in prior cold winters SLIMCAT tended to underestimate observed chemical ozone losses [Weber *et al.*, 2000; Sinnhuber *et al.*, 2000]. It is believed that denitrification in the model is generally underestimated [Guirlet *et al.*, 2000; Sinnhuber *et al.*, 2000]. However, during this winter UKMO analysis temperatures were low enough to permit large scale denitrification to occur in the model. Large scale denitrification allows chlorine activation to persist longer into early spring [Wagner *et al.*, 2001, 2002] leading to continued chemical ozone loss well into March [Sinnhuber *et al.*, 2000].

7. Midlatitude Ozone Loss

[42] Usually a small fraction of vortex air is eroded off the vortex before the final breakup [Norton *et al.*, 1995]. This air can be depleted in ozone and can contribute to the observed midlatitude ozone trend [see, e.g., Randel *et al.*, 1999; Bodeker *et al.*, 2001]. Most of the ozone dilution in midlatitudes occurs around the time of the vortex breakup [Knudsen *et al.*, 1998b]. In the Arctic the vortex is much less stable and the breakup happens earlier than in the Antarctic. Strong dynamical wave forcing in the Northern Hemisphere can lead to significant mixing of polar air into midlatitudes [Hood *et al.*, 1999]. The photochemical replacement time in the extratropical lower stratosphere is sufficiently long that it plays no role in the recovery of ozone [Knudsen *et al.*, 1998b]. Dilution thus may have a substantial impact on year-round trends (see Figure 2).

[43] Figure 9 shows the mean ozone vmr at 475 K isentropic level for the 20–30 PVU range, which is the region just outside the vortex edge region. There appears a small decrease in outer vortex ozone vmr averaged over the

20–30 PVU range after day 60. Comparison with passive ozone tracer data from SLIMCAT shows a net chemical loss of 0.3 ppmv between day 4 (4 January) and day 100 (10 April) as shown by the difference between passive ozone and GOME on day 100. While the passive ozone remains constant between day 4 and day 47 (17 February) a small increase of about 0.3 ppmv is observed by GOME. In late February GOME ozone decreases again to its initial value on day 100. This coincides with the period of increased outflow of polar vortex air in midlatitudes as shown in top of Figure 5. However, passive ozone increases until day 100 (Figure 6) by about 0.2 ppmv. Adding both numbers, one arrives at a chemical ozone loss contribution of 0.5 ppmv between day 45 and day 100. The latter number should be only considered as an upper limit. A chemical ozone loss of 0.3 ppmv for the longer period amounts to a chemical ozone loss of about 12% in the 20–30 PVU range at 475 K. The uncertainty is of the same order since the standard deviations for the daily ozone mean value ranges between 0.3 and 0.5 ppmv (Figure 9). CTMs show differences in transport and residual circulation, such that the error in passive ozone adds another uncertainty to our estimate [Bregman *et al.*, 2001; Hall *et al.*, 1999]. The loss estimate stated here is therefore not statistically significant.

8. Conclusions

[44] In this paper, we presented vortex-averaged chemical ozone loss calculations derived from height resolved ozone measurements from GOME. The method to include diabatic correction to separate dynamical and chemical contribution to ozone change has been applied to the GOME satellite data for the first time. For the period 25 January to 13 March a mean chemical ozone depletion rate of 43 ppbv/d at 475 K isentropic level was derived amounting to a total chemical loss of 1.8 ± 0.4 ppmv (49%) during this period. The largest uncertainty comes from the accuracy of the GOME ozone vmr at the starting date since only few measurements were available inside the polar vortex. The agreement between GOME and sonde measurements and, on the other hand, with the SLIMCAT 3-D chemical transport model is very good except for the period after mid-March when the vortex became strongly distorted causing a positive bias in the GOME data. Apparently the low vertical resolution in the GOME measurements leads to contributions of nonvortex air at other altitudes to contribute to the observed isentropic ozone vmr after mid-March. Furthermore GOME generally underestimates the loss confined to a small vertical region. The amount of chemically destroyed ozone in the column 400–600 K was 73 ± 11 DU for the period 12 February and 13 March 2000 and 114 ± 11 DU for the 25 January to 13 March period. These results are consistent with other measurements in that winter. The GOME data are well suited for investigating the contribution of polar losses to midlatitude ozone. Within the potential vorticity range of 20–30 PVU a contribution of 12% to midlatitude chemical ozone loss at 475 K isentropic level until day 100 was found from differences to passive ozone from SLIMCAT. These losses were most likely due to dilution effects during the breakup of the polar vortex. Since the uncertainties in residual circulation and transport in models can be quite significant, this midlatitude ozone loss is not statistically significant. Further

studies are under way to extend this type of studies to other Arctic winters.

[45] **Acknowledgments.** Part of this work was supported by the EU project EUROSOLVE/THESEO 2000, the University of Bremen, and the State Bremen. We thank the German Remote Sensing Data Center (DFD) of the DLR in Oberpfaffenhofen, Germany, for providing the GOME operational total ozone column version 2.7 and calibrated level 1 spectral data version 2.0. We thank K. Shine for providing the MIDRAD model used in the heating rate calculations. The provision of Arctic sonde data by Geir Braathen, NILU, is gratefully acknowledged. SLIMCAT data have been kindly provided by Adrian Lee, University of Cambridge, and Björn-Martin Sinnhuber and Martyn Chipperfield, University of Leeds. The UK Meteorological Office and the European Centre for Medium-Range Weather Forecast are thanked for providing the meteorological data sets. We thank the NASA/GSFC Atmospheric Chemistry branch for providing TOMS/EP version 7 data.

References

- Bevilacqua, R. M., et al., POAM II ozone observations in the Antarctic ozone hole in 1994, 1995, and 1996, *J. Geophys. Res.*, **102**, 23,643–23,657, 1997.
- Bhartia, P. K., R. D. McPeters, C. L. Mateer, L. E. Flynn, and C. Wellemeyer, Algorithm for estimation of vertical ozone profiles from back scattered ultraviolet technique, *J. Geophys. Res.*, **101**, 18,793–18,806, 1996.
- Bodeker, G. E., J. C. Scott, K. Kreher, and R. L. McKenzie, Global ozone trends in potential vorticity coordinates using TOMS and GOME inter-compared against the Dobson network: 1978–1998, *J. Geophys. Res.*, **106**, 23,029–23,042, 2001.
- Braathen, G. O., M. Rummikainen, E. Kyrö, U. Schmidt, A. Dahlback, T. S. Jorgensen, R. Fabian, V. V. Rudagov, M. Gil, and R. Borchers, Temporal development of ozone within the Arctic vortex during the winter of 1991/1992, *Geophys. Res. Lett.*, **21**, 1407–1410, 1994.
- Bramstedt, K., GOME Ozonprofile: Weiterentwicklung und Validierung, Ph.D. thesis, Univ. of Bremen, Bremen, Germany, 2001.
- Bramstedt, K., K.-U. Eichmann, M. Weber, V. Rozanov, and J. P. Burrows, GOME ozone profiles: A global validation with HALOE Measurements, *Adv. Space Res.*, **29**(11), 1637–1642, 2002.
- Bregman, A., M. C. Krol, H. Teyssedre, W. A. Norton, A. Iwi, M. Chipperfield, G. Pitari, J. K. Sundet, and J. Lelieveld, Chemistry-transport model comparison with ozone observations in the midlatitude lowermost stratosphere, *J. Geophys. Res.*, **106**, 17,479–17,496, 2001.
- Bremer, H., M. von König, A. Kleinböhl, H. Küllmann, K. Künzi, K. Bramstedt, J. P. Burrows, and K.-U. Eichmann, Ozone depletion observed by Airborne Submillimeter Radiometer during the Arctic winter 1999/2000, *J. Geophys. Res.*, **107**, doi:10.1029/2001JD000546, in press, 2002.
- Burrows, J. P., A. Dehn, B. Deters, S. Himmelmann, A. Richter, S. Voigt, and J. Orphal, Atmospheric remote-sensing reference data from GOME, 1, Temperature-dependent absorption cross-sections of NO₂ in the 231–794 nm range, *J. Quant. Spectrosc. Radiat. Transfer*, **60**, 1025–1031, 1998.
- Burrows, J. P., et al., The Global Ozone Monitoring Experiment (GOME): Mission concept and first scientific results, *J. Atmos. Sci.*, **56**, 151–175, 1999a.
- Burrows, J. P., A. Richter, A. Dehn, B. Deters, S. Himmelmann, S. Voigt, and J. Orphal, Atmospheric remote-sensing reference data from GOME, 2, Temperature-dependent absorption cross-sections of O₃ in the 231–794 nm range, *J. Quant. Spectrosc. Radiat. Transfer*, **61**, 509–517, 1999b.
- Chance, K. V., J. P. Burrows, D. Perner, and W. Schneider, Satellite measurements of atmospheric ozone profiles, including tropospheric ozone, from ultraviolet/visible measurements in the nadir geometry: A potential method to retrieve tropospheric ozone, *J. Quant. Spectrosc. Radiat. Transfer*, **57**, 5224–5230, 1997.
- Chipperfield, M. P., Multiannual simulations with a three-dimensional chemical transport model, *J. Geophys. Res.*, **104**, 1781–1805, 1999.
- Chipperfield, M. P., and R. L. Jones, Relative influences of atmospheric chemistry and transport on Arctic ozone trends, *Nature*, **400**, 551–554, 1999.
- Chipperfield, M. P., and J. A. Pyle, Model sensitivity studies of Arctic ozone depletion, *J. Geophys. Res.*, **103**, 28,389–28,403, 1998.
- Coy, L., E. R. Nash, and P. A. Newman, Meteorology of the polar vortex: Spring 1997, *Geophys. Res. Lett.*, **24**, 693–696, 1997.
- de Beek, R., R. Hoogen, V. V. Rozanov, and J. P. Burrows, Ozone profile retrieval from GOME satellite data, 1, Algorithm description, *Rep. ESA-SP414*, pp. 749–754, Eur. Space Agency, ESA/ESTEC, Noordwijk, Netherlands, 1997.
- Eichmann, K.-U., K. Bramstedt, M. Weber, V. V. Rozanov, R. Hoogen, and J. P. Burrows, O₃ profiles from GOME satellite data, II, Observations in the Arctic spring 1997 and 1998, *Phys. Chem. Earth*, **24**, 453–457, 1999.
- Fortuin, J. P. F., and H. M. Kelder, An ozone climatology based on ozone sonde and satellite measurements, *J. Geophys. Res.*, **103**, 31,709–31,719, 1998.
- Guirlet, M., M. P. Chipperfield, J. A. Pyle, F. Goutail, J. P. Pommereau, and E. Kyrö, Modeled Arctic ozone depletion in winter 1997/1998 and comparison with previous winters, *J. Geophys. Res.*, **103**, 22,185–22,200, 2000.
- Hall, T. M., D. W. Waugh, K. A. Boering, and R. A. Plumb, Evaluation of transport in stratospheric models, *J. Geophys. Res.*, **104**, 18,815–18,839, 1999.
- Harris, N. R. P., M. Rex, F. Goutail, B. M. Knudsen, G. L. Manney, R. Müller, and P. von der Gathen, Comparison of empirically derived ozone losses in the Arctic vortex, *J. Geophys. Res.*, **107**, 8264, doi:10.1029/2001JD000482, 2002.
- Hauchecorne, A., and T. Peter, Mid-latitude and tropical ozone, in *European Research in the Stratosphere 1996–2000: Advances in Our Understanding of the Ozone Layer During THESEO*, pp. 133–189, chap. 4, Eur. Comm., 2001.
- Hood, L., S. Rossi, and M. Beulen, Trends in lower stratospheric zonal winds, Rossby wave breaking behavior, and column ozone at northern midlatitudes, *J. Geophys. Res.*, **104**, 24,321–24,339, 1999.
- Hoogen, R., V. Rozanov, and J. P. Burrows, Ozone profiles from GOME satellite data: Algorithm description and first validation, *J. Geophys. Res.*, **104**, 8263–8280, 1999a.
- Hoogen, R., V. V. Rozanov, K. Bramstedt, K.-U. Eichmann, M. Weber, and J. P. Burrows, Ozone profiles from GOME satellite data, I, Comparison with ozone sonde measurements, *Phys. Chem. Earth*, **24**, 447–452, 1999b.
- Hoppel, K., R. Bevilacqua, G. Nedoluha, C. Deniel, F. Lefevre, J. Lumpe, M. Fromm, C. Randall, J. Rosenfield, and M. Rex, POAM III observations of Arctic ozone loss for the 1999/2000 winter, *J. Geophys. Res.*, **107**, 8262, doi:10.1029/2001JD000476, 2002.
- Klein, U., I. Wohltmann, K. Lindner, and K. F. Künzi, Ozone depletion and chlorine activation in the Arctic winter 1999/2000 observed in Ny-Ålesund, *J. Geophys. Res.*, **107**, doi:10.1029/2001JD000543, in press, 2002.
- Kneizys, F. X., E. P. Shettle, L. W. Abreu, J. H. Chetwynd, G. P. Anderson, W. O. Gallery, J. E. A. Selby, and S. A. Clough, *Users Guide to LOW-TRAN7*, Tech. Rep. AFGL-TR-88-0177, Air Force Geophys. Lab., Bedford, Mass., 1988.
- Knudsen, B. M., et al., Ozone depletion in and below the Arctic vortex for 1997, *Geophys. Res. Lett.*, **25**, 627–630, 1998a.
- Knudsen, B. M., W. A. Lahoz, and J. J. Morcrette, Evidence for a substantial role for dilution in northern mid-latitude ozone depletion, *Geophys. Res. Lett.*, **25**, 4501–4504, 1998b.
- Kozlov, V., Design of experiments related to the inverse problem of mathematical physics (in Russian), in *Mathematical Theory of Experiment Design*, edited by C. M. Ermakov, pp. 216–246, Nauka, Moscow, 1983.
- Lait, L., et al., Ozone loss from quasi-conservative coordinate mapping during the 1999/2000 SOLVE/THESEO 2000 campaigns, *J. Geophys. Res.*, **107**, doi:10.1029/2001JD000998, in press, 2002.
- Lambert, J.-C., M. van Roozendaal, M. de Maziere, P. C. Simon, J.-P. Pommereau, F. Goutail, A. Sarkissian, and J. F. Gleason, Investigation of pole-to-pole performances of space-borne atmospheric chemistry sensors with the NDSC, *J. Atmos. Sci.*, **56**, 176–193, 1999.
- Manney, G. L., and J. L. Sabutis, Development of the polar vortex in the 1999/2000 Arctic winter stratosphere, *Geophys. Res. Lett.*, **27**, 2589–2592, 2000.
- Manney, G. L., L. Froidevaux, J. W. Waters, M. L. Santee, W. G. Read, D. A. Flower, R. F. Jarrot, and R. W. Zurek, Arctic ozone depletion observed by UARS MLS during the 1994–1995 winter, *Geophys. Res. Lett.*, **23**, 85–88, 1996.
- Müller, R., P. J. Crutzen, J.-U. Groo's, C. Brühl, J. M. Russell, H. Gerand, and D. S. McKenna, Severe chemical ozone loss in the Arctic during the winter of 1995–1996, *Nature*, **389**, 709–712, 1997.
- Newman, P. A., J. F. Gleason, R. D. McPeters, and R. S. Stolarski, Anomalous low ozone over the Arctic, *Geophys. Res. Lett.*, **24**, 2689–2692, 1997.
- Newman, P. A., et al., An overview of the SOLVE/THESEO 000 campaign, *J. Geophys. Res.*, **107**, doi:10.1029/2001JD001303, in press, 2002.
- Pawson, S., and B. Naujokat, The cold winters of the middle 1990s in the northern lower stratosphere, *J. Geophys. Res.*, **104**, 14,209–14,222, 1999.
- Platt, U., and D. Perner, Differential optical absorption spectroscopy, in *Air Monitoring by Spectroscopic Techniques*, vol. 127, edited by M. Siegrist, pp. 27–84, John Wiley, New York, 1994.
- Proffitt, M. H., K. Aikin, J. J. Margitan, M. Loewenstein, J. R. Podolske, A. Weaver, K. R. Chan, H. Fast, and J. W. Elkins, Ozone loss inside the

- northern polar vortex during the 1991–1992 winter, *Science*, 261, 1150–1154, 1993.
- Randel, W. J., F. Wu, J. M. Russell III, A. Roche, and J. W. Waters, Seasonal cycles and QBO variations in vtratospheric CH₄ and H₂O observed in UARS HALOE data, *J. Atmos. Sci.*, 55, 163–185, 1998.
- Randel, W. J., R. S. Stolarski, D. M. Cunnold, J. A. Logan, M. J. Newchurch, and J. M. Zawodny, Trend in the vertical distribution of ozone, *Science*, 285, 1689–1692, 1999.
- Rex, M., N. R. P. Harris, P. von der Gathen, R. Lehmann, G. O. Braathen, E. Reimer, and A. Beck, Prolonged stratospheric ozone loss in the 1995/96 Arctic winter, *Nature*, 389, 835–838, 1997.
- Rex, M., et al., Chemical depletion of Arctic ozone in winter 1999/2000, *J. Geophys. Res.*, 107, doi:10.1029/2001JD000533, in press, 2002.
- Rodgers, C. D., Inverse methods for atmospheric sounding: Theory and practice, in *Series on Atmospheric, Oceanic and Planetary Physics*, vol. 2, World Sci., River Edge, N.J., 2000.
- Rozanov, V. V., D. Diebel, R. J. D. Spurr, and J. P. Burrows, GOMETRAN: A radiative transfer model for the satellite project GOME, the plane-parallel version, *J. Geophys. Res.*, 102, 16,683–16,695, 1997.
- Rozanov, V. V., T. Kurosu, and J. P. Burrows, Retrieval of atmospheric constituents in the UV-visible: A new quasi-analytical approach for the calculation of weighting functions, *J. Quant. Spectrosc. Radiat. Transfer*, 60, 277–299, 1998.
- Schoeberl, M. R., et al., An assessment of the ozone loss during the SOLVE/THESEO 2000 Arctic campaign, *J. Geophys. Res.*, 107, doi:10.1029/2001JD000412, in press, 2002.
- Shine, K. P., On the cause of the relative greenhouse strength of gases such as the halocarbons, *J. Atmos. Sci.*, 48, 1513–1518, 1991.
- Singer, S. F., and R. C. Wentworth, A method for the determination of the vertical ozone distribution from a satellite, *J. Geophys. Res.*, 62, 299–308, 1957.
- Sinnhuber, B.-M., J. Langer, U. Klein, U. Raffalski, and K. Künzi, Ground based millimeter-wave observations of Arctic ozone depletion during winter and spring of 1996/97, *Geophys. Res. Lett.*, 25, 3227–3330, 1998.
- Sinnhuber, B.-M., et al., Large loss of total ozone during the Arctic winter of 1999/2000, *Geophys. Res. Lett.*, 27, 3473–3476, 2000.
- Sobel, A. H., R. A. Plumb, and D. W. Waugh, Methods of calculating isentropic transport across the polar vortex edge, *J. Atmos. Sci.*, 54, 2241–2260, 1997.
- Swinbank, R., and A. O'Neill, A stratosphere-troposphere data assimilation system, *Mon. Weather Rev.*, 122, 686–702, 1994.
- von der Gathen, P., et al., Observational evidence for chemical ozone depletion over the Arctic in winter 1991–92, *Nature*, 375, 131–134, 1995.
- Wagner, T., C. Leue, K. Pfeilsticker, and U. Platt, Monitoring of the stratospheric chlorine activation by GOME OCIO measurements in the austral and boreal winters 1995 through 1999, *J. Geophys. Res.*, 106, 4971–4986, 2001.
- Wagner, T., F. Wittrock, A. Richter, M. Wenig, J. P. Burrows, and U. Platt, Continuous monitoring of the high and persistent chlorine activation during the Arctic winter 1999/2000 by the GOME instrument on ERS-2, *J. Geophys. Res.*, 107, doi:10.1029/2001JD000466, in press, 2002.
- Waibel, A. E., et al., Arctic ozone loss due to denitrification, *Science*, 283, 3327–3330, 1999.
- Weber, M., J. P. Burrows, and R. P. Cebula, GOME Solar UV/VIS irradiance measurements between 1995 and 1997—First results on proxy solar activity studies, *Sol. Phys.*, 77, 63–77, 1998.
- Weber, M., K.-U. Eichmann, K. Bramstedt, J. P. Burrows, A. Lee, and B.-M. Sinnhuber, Vertical ozone distribution in the Northern Hemisphere in late winter/early spring between 1996/97 and 1999/2000: GOME satellite observation of Arctic chemical ozone loss in the lower stratosphere and comparison with the 3D chemical transport model SLIMCAT, in *Proceedings of the Quadrennial Ozone Symposium, Sapporo, 3–8 July 2000*, pp. 105–106, Nat. Space Devel. Agency of Jpn., Tokyo, 2000.
- Weber, M., K.-U. Eichmann, F. Wittrock, K. Bramstedt, L. Hild, A. Richter, J. P. Burrows, and R. Müller, The cold Arctic winter 1995/96 as observed by the Global Ozone Monitoring Experiment GOME and HALOE: Tropospheric wave activity and chemical ozone loss, *Q. J. R. Meteorol. Soc.*, in press, 2001.

K. Bramstedt, J. P. Burrows, K.-U. Eichmann, and M. Weber, Institute of Environmental Physics, University of Bremen, Kufsteiner Strasse, 28359 Bremen, Germany. (bram@iup.physik.uni-bremen.de; burrows@iup.physik.uni-bremen.de; eichmann@iup.physik.uni-bremen.de; weber@uni-bremen.de)